Pro-oxidant properties of indolone-*N*-oxides in relation to their antimalarial properties

Nguyen Thi Hoang Yen [a,b,c], Hany Ibrahim [a,b,*], Karine Reybier [a,b], Pierre Perio [a,b], Florence Souard [a,b], Ennaji Najahi [a,b], Paul-Louis Fabre [d,e], Francoise Nepveu [a,b]

[a] *Université de Toulouse, UPS, UMR 152 PHARMA-DEV, 118 route de Narbonne, F-31062 Toulouse cedex 9, France*
[b] *IRD, UMR 152, F-31062 Toulouse cedex 9, France*
[c] *Medicine and Pharmacy University of Ho Chi Minh City, 41 Dinh Tien Hoang Street, District 1, Ho Chi Minh City, Viet Nam*
[d] *Université de Toulouse, UPS, UMR 5503 Laboratoire de Génie Chimique, F-31062 Toulouse cedex 9, France*
[e] *CNRS, UMR 5503; F-31062 Toulouse cedex 9, France*

Keywords:
Pro-oxidant drugs
Indolone-*N*-oxides
Antimalarial drugs
Cyclic voltammetry
Electron paramagnetic resonance (EPR)

A B S T R A C T

Indolone-*N*-oxides (INODs) are bioreducible and possess remarkable anti-malarial activities in the low nanomolar range in vitro against different *Plasmodium falciparum* (*P. falciparum*) strains and in vivo. INODs have an original mechanism of action: they damage the host cell membrane without affecting non-parasitized erythrocytes. These molecules produce a redox signal which activates SYK tyrosine kinases and induces a hyperphosphorylation of AE1 (band 3, erythrocyte membrane protein). The present work aimed to understand the early stages of the biochemical interactions of these compounds with some erythrocyte components from which the redox signal could originate. The interactions were studied in a biomimetic model and compared with those of chloroquine and artemisinin. The results showed that INODs i) do not enter the coordination sphere of the metal in the heme iron complex as does chloroquine; ii) do not generate iron-dependent radicals as does artemisinin; iii) generate stable free radical adducts after reduction at one electron; iv) cannot trap free radicals after reduction. These results confirm that the bioactivity of INODs does not lie in their spin-trapping properties but rather in their pro-oxidant character. This property may be the initiator of the redox signal which activates SYK tyrosine kinases.

1. Introduction

Molecular and proteic redox systems play an important role in the control of cellular homeostasis and antioxidant defenses. Some drugs containing a redox pharmacophore (quinone and quinoid compounds, *N*-oxide, nitro and thiol derivatives, endoperoxides) may generate an oxidative stress in the cell that can be fatal for the hosted microbes and for the cells. We recently reported that indolone-*N*-oxide derivatives (INODs), which are bioreducible, possess remarkable anti-malarial activities in the low nanomolar range in vitro against different *Plasmodium falciparum* (*P. falciparum*) strains and are also active in vivo [1,2]. Moreover, these compounds are only cytotoxic at very high doses (micromolar range) thus giving a very interesting selectivity index. Early studies showed that INODs have redox potentials near to those of 1,4-quinones and therefore may exert their biological action by oxidizing essential biomolecules [3]. In addition, they contain a nitrone function that may react with the glutathiyl radical formed within the cells upon oxidation of glutathione [4]. To explore the mechanism of action of INODs, we screened for changes in INOD-treated *P. falciparum*-infected red blood cells (RBCs) using a comprehensive proteomic approach. INODs have an original mechanism of action: they damage the host cell membrane, without affecting non-parasitized erythrocytes, with the consequent RBC membrane vesiculation and destabilization responsible for parasite death. The mechanism leading to the selective destabilization of the membrane of parasitized erythrocytes involves the activation of a stress responsive phosphorylation pathway which finally induces the uncoupling of membrane-cytoskeleton interactions. Marked hyperphosphorylation of AE1 (band 3) appears to be the hallmark of the process [5]. We have also studied the kinetics of penetration and biotransformation of these molecules in the erythrocytes. The compounds penetrate very rapidly, accumulate and are rapidly bio-transformed in the RBC cytosol by a thiol-dependent reduction possibly via an enzymatic pathway [6]. Because INODs contain the *N*-oxide functional group, this bioreductive transformation was expected, as it had previously been described for other *N*-oxides derivatives [7]. We recently reported the examination of the antimalarial properties of these compounds in relation to their redox properties using cyclic voltammetry coupled to EPR spectroscopy [8]. Given the redox events occurring in *Plasmodium* infected RBCs, this

* Corresponding author at: Université de Toulouse, UPS, UMR 152 PHARMA-*DEV*, 118 route de Narbonne, F-31062 Toulouse cedex 9, France. Tel.: +33 562256870; fax: +33 562259802.
E-mail address: hanygamal85@hotmail.com (H. Ibrahim).

bioreductive transformation may be pivotal for the parasite redox balance and for the antiplasmodial activity. Altogether these studies showed that these compounds target the redox metabolism of the infected host cell.

In a previous study [2] we investigated the in vitro antimalarial properties of compound **1** (6-(4-chlorophenyl)-7*H*-[1,3]dioxolo [4,5-f]indol-7-one-5-oxide) against fresh clinical isolates of *P. falciparum*. This study was carried out to (i) compare the activity of compound **1** with that of chloroquine (CQ) and artemisinin (ART) to assess the potential for cross-resistance, (ii) investigate drug interactions of indolone-*N*-oxides with standard antimalarials and (iii) determine the stage-dependent activity of indolone-*N*-oxides. Compound **1** was equipotent against chloroquine-susceptible and chloroquine-resistant isolates. There was no correlation between responses to chloroquine and compound **1** ($r = 0.015$; $P > 0.05$), but the in vitro responses of compound **1** and dihydroartemisinin were significantly and positively correlated ($r = 0.444$; $P < 0.05$). INODs, as well as artemisinin, inhibited parasite maturation at the ring stage. The antimalarials, chloroquine and artemisinin, also target the redox metabolism of *P. falciparum*. The former belongs to the quinolines that interfere with hemoglobin biocrystallization [9] preventing hemozoin formation, while artemisinin-like derivatives create oxidative stress by generating radical intermediates [10]. Considering i) the mechanisms of action of artemisinin and chloroquine; ii) the redox properties of INODs; iii) and the interactions observed between these molecules in fresh clinical isolates [2], the present study aimed to understand the early stages of the biochemical interactions of the INODs with some RBC components and to compare them with the actions of chloroquine and artemisinin, in biomimetic models. As the lead compound of the INOD series, compound **1** was selected for these studies (Fig. 1). EPR and electrochemical experiments were designed to study i) the bioreductive properties of compound **1** in relation to those of ART and CQ; ii) the interaction with non-protein thiols (L-cysteine and glutathione); iii) the capacity to interact with heme; iv) the capacity to generate and/or trap radicals.

2. Material and methods

2.1. Chemicals

6-(4-Chlorophenyl)-7*H*-[1,3]dioxolo[4,5-f]indol-7-one-5-oxide (compound **1**) was synthesized in our laboratory as previously reported [1]. Ferrous ammonium sulfate, hemin chloride, hydroxylamine hydrochloride ($NH_2OH.HCl$), sodium acetate, sodium dihydrogen phosphate (NaH_2PO_4), di-sodium hydrogen phosphate (Na_2HPO_4) and ferrocene were purchased from Prolabo (VWR, France); dimethyl sulfoxide (DMSO), HCl 37%, NaOH, tris-HCl, hydrogen peroxide (H_2O_2), L-cysteine (L-Cys), anhydrous acetonitrile (ACN), ferrocene, chloroquine diphosphate salt, artemisinin, and glutathione (GSH) were purchased from Sigma-Aldrich (St. Quentin, France); EDTA and tetrabutyl ammonium perchlorate (TBAP) were purchased from Fluka, RPMI from Cambrex (Verviers, Belgium).

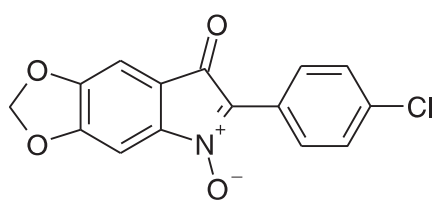

Fig. 1. Structure of compound **1**.

2.2. Electrochemical and chemical analysis

2.2.1. Electrochemical analysis

Experiments were carried out at 25 °C (thermal bath) in DMSO/Tris–HCl buffer (0.1 M) (80/20, v/v), using a Voltalab 80 PGZ 402 (Radiometer) with a conventional three-electrode system including an Ag/AgCl electrode or an saturated calomel electrode (SCE) as the reference electrode, a platinum electrode (5 × 5 mm) as the counter electrode and a glassy carbon disk (1 mm diameter) as the working electrode. All solutions were deoxygenated by passing a gentle constant stream of pre-purified argon through the solution for 10 min and maintaining a blanket of the inert gas over the solution during the experiment. The glassy carbon electrode was cleaned after each run by electrochemical cleaning to avoid aggressive changes. The electrochemical cleaning process was done in acetate buffer pH 4.5 by polarization for 10 min at −500 mV then at 2000 mV vs. the reference electrode (the electrochemical cleaning process was done according to the Princeton Co protocol). Between experiments, glassy carbon was rubbed on the polishing pad with blue diamond slurry particles (Waters, USA), then washed with methanol and distilled water.

2.2.2. Chemical analysis of the interaction between compound 1 and L-Cys

Liquid chromatography (LC) coupled to mass spectrometry (MS) analysis was carried out with an LC-PDA-MS^n system (Thermo Electron Corporation and Spectra System (SS)) including an automatic injector with an oven (SS-AS3000), a degasser (SS-SCM1000), and a quaternary pump (SS-P1000 XR) coupled to a photodiode array detector PDA (SS-UV6000LP), and an ion trap mass spectrometer (Finnigan LCQ Deca XP Max). Nitrogen was used as a nebulizing and drying gas. Data acquisition was carried out using Finnigan Xcalibur software (version 1.4). The atmospheric pressure chemical ionization (APCI) source was used in the negative ion mode. Mass scans were done in the range *m/z* 50–650. The chromatographic separation was done on an analytical column Luna® C-18 (5 μm, 250 mm × 4.6 mm) using a C-18 pre-column (5 μm, 4.6 mm × 3 mm) (Phenomenex, France). The separation was done in gradient mode using solvent A (water) and solvent B (CH_3OH). The gradient program was the following: at $t = 0$–3 min; solvents (95% A/5% B, v/v); at $t = 4$–20 min, solvents (15% A/85% B, v/v); at $t = 22$ min, solvents (95% A/5% B, v/v); the column regeneration time was 10 min and the mobile phase flow rate was 1 ml/min. The analysis was performed at room temperature (RT), with 20 μl of sample injected. Compound **1** was dissolved in DMSO and L-Cys in phosphate buffer and they were mixed to give a final concentration of 0.25 and 2.5 mM for compound **1** and L-Cys, respectively.

2.3. Electron paramagnetic resonance (EPR) experiments

EPR spectra were obtained at X-band on a Brüker EMX-8/2.7 (9.86 GHz) equipped with a high-sensitivity cavity (4119/HS 0205) and a gaussmeter (Bruker, Wissembourg, France). EPR data processing and spectrum computer simulation were performed using WINEPR and SIMFONIA software (Bruker, Wissembourg, France).

2.3.1. Interaction with heme

Compound **1**, artemisinin and chloroquine were each incubated under an argon atmosphere with hemin or heme obtained by reducing hemin with $NH_2OH.HCl$. The analyzed samples were prepared in DMSO by mixing hemin/compound at the stoichiometric ratio 1/4 (0.75/3 mM) or hemin/$NH_2OH.HCl$/compound at the stoichiometric ratio 1/10/4 (0.75/7.5/3 mM). The solutions were stirred at room temperature for 5 h before recording the EPR spectra. The recording was carried out at 107 K using a liquid nitrogen flow in a quartz tube (inner diameter: 4 mm) containing 250 μL analyzed solution. Typical scanning parameters were: scan rate, 0.6 G/s; scan number, 1; modulation amplitude, 5.10^{-4} G; modulation frequency, 100 kHz,

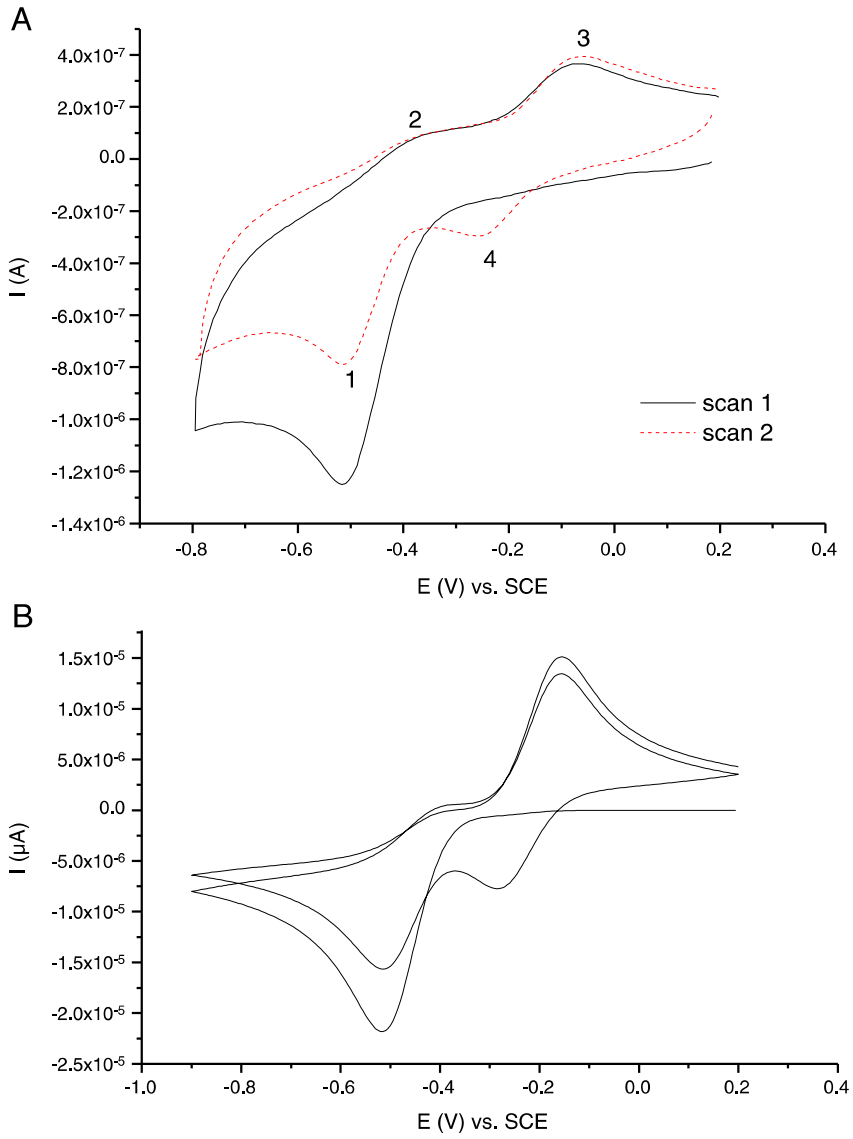

Fig. 2. A) cyclic voltammograms at a glassy carbon electrode (1 mm diameter) in DMSO/water (80/20 v/v) of compound **1** (10 µM), potential scan speed 0.1 V/s; B) the corresponding simulated voltammograms (DigiElch 6.F (Gamry)).

microwave power, 20.2 mW; time constant, 20.48 ms, sweep width, 5000 G receiver gain, 68.

2.3.2. EPR spectroelectrochemical analysis

For spectro-electrochemical measurements, the EPR spectrometer was coupled to a potentiostat-galvanostat (EG&G Princeton Applied Research-Model 362). A flat quartz cell adapted to electrochemical measurements (Bruker, Wissembourg, France) was used for analysis. The electrochemical reduction was carried out using a three-electrode set-up: the working and counter-electrode were platinum and the reference electrode was a silver wire. The applied potential was chosen to be on the diffusion plateau of the first reduction wave obtained under stationary conditions: $E_{applied} = -0.9$ V. The electrolysis potential was applied for 5 min to the solution containing the compound in

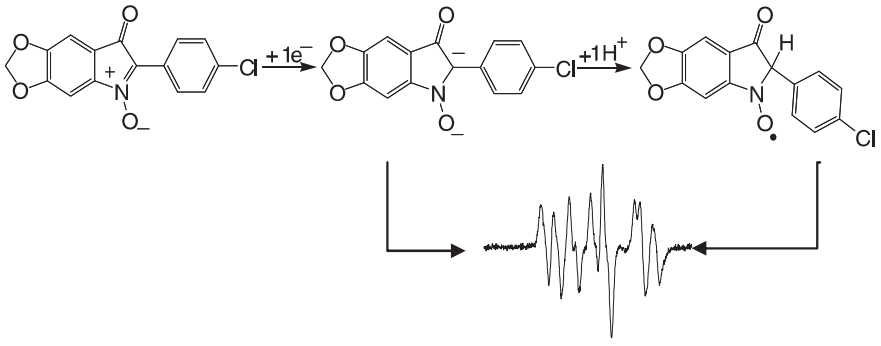

Scheme 1. Relationship between the reduced forms of compound **1** and the corresponding EPR spectra.

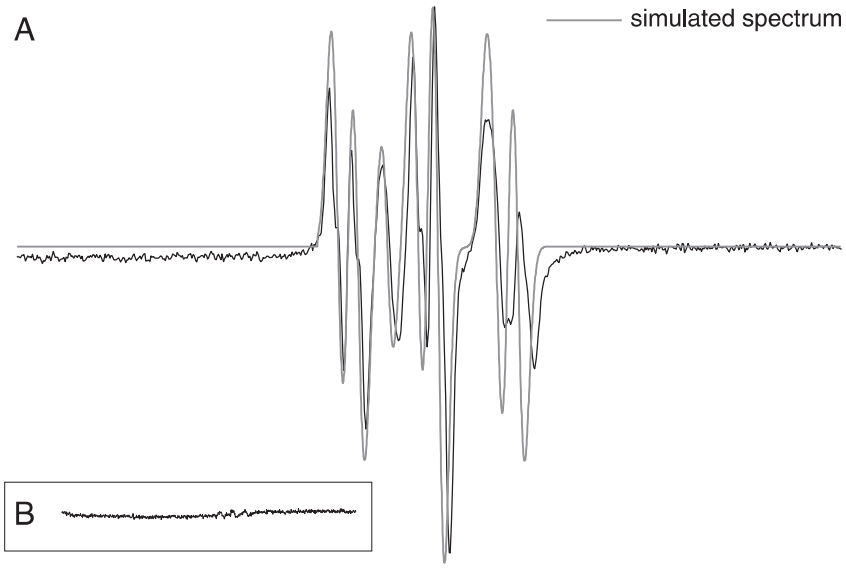

Fig. 3. EPR spectra of the reduced form of compound **1**: EPR spectra and the corresponding simulated spectra recorded during the electrolysis at −0.9 V vs. SCE in DMSO/water (80/20, v/v) containing TBAP (100 mM) in the absence (A), and in the presence, inset (B), of L-cysteine (100 mM).

acetonitrile/TPAB and the EPR spectrum was immediately recorded as a function of time. Typical scanning parameters were: scan rate, 1.2 G/s; scan number, 1; modulation amplitude, 1 G; modulation frequency, 100 kHz; microwave power, 20 mW; sweep width, 105 G; sweep time, 83.88 s; time constant, 40.96 ms; receiver gain, 5×10^4.

2.3.3. Interaction of INOD with radicals derived from artemisinin and iron

The compound was dissolved in DMSO to obtain a 3 mM stock solution. EPR spectra were recorded in DMSO/water 90/10 (v/v) with the final concentrations: artemisinin 2.5 mM, $Fe^{2+}((NH_4)_2Fe(SO_4)_2.6H_2O)$ 0.25 mM and compound **1** 0.25 mM. The final solution was vortexed for 15 s and then transferred into the quartz flat cell (FZK160-5 × 0.3; Magnettech). Typical scanning parameters were: scan rate 0.6 G/s, scan number 10, modulation amplitude 1 mG, modulation frequency 100 kHz, microwave power 20 mW, spectrum width 5000 G, gain 80, frequency 9.86×10^9 Hz, magnetic field sweep width 150 G, sweep time 41.94 ms, time constant 20.48 ms, receiver gain 2×10^5, 10 scans.

3. Results and discussion

3.1. Electrochemical behavior of compound **1** *and interaction with thiol compounds*

The use of electrochemical methods to obtain relevant information about drugs containing a redox pharmacophore is particularly important to predict their biotransformation in cells. The main structural feature of INODs is the redox heterocyclic core (redox pharmacophore) in which the nitrone moiety ($C = N^+ - O^-$) is conjugated to the ketone function giving to the molecule the capabilities to undergo several oxidation–reduction reactions.

The electrochemical behavior of this kind of compounds has been previously reported in non-aqueous media [8,11]. In this work, the reducible behavior of INODs was studied in presence of water using cyclic voltammetry. Due to their low aqueous solubility, INODs were studied in DMSO/water 80/20 (v/v). This solvent mixture was selected after testing different solvent systems (ex. ACN/H_2O; dimethyl formamide/H_2O). The system selected (DMSO/H_2O) was the best compromise to simultaneously solubilize INOD compounds and L-Cys (or GSH) where other systems had failed to do so. Fig. 2 represents the voltammograms obtained for compound **1**. The first cycle shows the reduction of the electroactive compound **1** around −0.5 V; on the backward scan, two anodic peaks are observed around −0.4 V and −0.1 V. In the second cycle and forward scan, a cathodic peak around −0.2 V appeared and is coupled with the anodic peak around −0.1 V. It appears that the electrochemical system of compound **1** can be translated by two electron transfers: $E_{1/2} = -0.43$ V and $E_{1/2} = -0.15$ V. The cathodic peak currents of the first cycle are linearly related to the square root of the potential scan rate as for a diffusion controlled process. By comparison with the oxidation peak current of ferrocene recorded under the same conditions, mono-electronic transfers are expected for the reductions of INODs. The electron transfer recorded during the first reduction process corresponds, as demonstrated in non-aprotic solvent [8], to the reduction of the *N*-oxide to a nitroxide radical-anion (Scheme 1). It can be noted that, by comparison with the voltammogram recorded in non-aqueous medium, the nitroxide function is more easily reduced in presence of water, due to the fact that electrochemical oxido-reduction requires higher energy when increasing the content of the organic phase in the solvent supporting electrolyte.

EPR spectro-electrochemical experiments were carried out in order to characterize the reduction products. The in-situ electrolysis ($E_{applied} = -0.9$ V vs. Ag/AgCl) was monitored by recording the EPR spectra. The EPR spectrum obtained at the beginning of the electrolysis (Fig. 3A) consists of a multi-lined pattern characteristic of the superposition of two species, the nitroxide radical-anion (three lined spectrum: $a_N = 6.27$ G, $a_H^\beta = 1$ G) and its protonated form (six lined spectrum: $a_N = 9.5$ G and $a_H^\beta = 2.3$ G) as demonstrated by the simulation presented in Fig. 3.

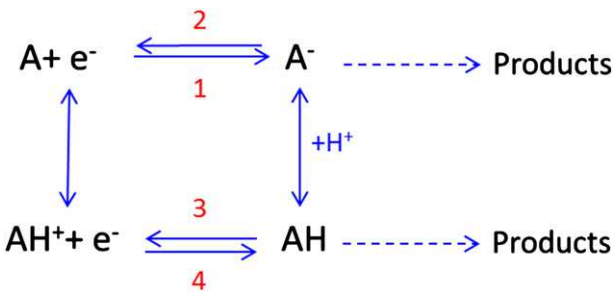

Scheme 2. Reductive pathway of compound **1**.

These results confirmed the expected monoelectronic transfer and the formation of two reduction products responsible, on the voltammogram, for the two oxidation peaks recorded (2 and 3) on the reverse scan and for the appearance of a second reduction wave (4) during the second scan. The reductive pathway of compound **1** (A) is presented in Scheme 2.

The reduction of compound **1** (A) gives the radical-anion A^- that is detected by EPR spectroscopy which is rapidly protonated into AH. On the backward scan, the oxidation peak of A^- is small ($Ep_2 \sim -0.4$ V) compared with that of the protonated AH ($Ep_3 \sim -0.06$ V). On the forward scan of the second cycle, the reduction of AH^+ is observed ($Ep_4 = -0.25$ V). Fig. 4 shows the normalized voltammograms ($I/v^{1/2}$ versus E) of the second cycle as a function of the potential scan rate. Due to the ohmic drop coming from the DMSO, the voltammograms shifted when the potential scan speed was increased. From Fig. 4, it can be seen that the oxidation peak of A^- ($Ep \sim -0.4$ V) did not increase with the potential scan rate, indicating a fast protonation. On the contrary, the normalized currents (anodic oxidation of AH or cathodic reduction of AH^+) increased with the potential scan speed because decomposition of AH is restricted and AH^+ is a weak acid.

Simulations with DigiElch 6.F (Gamry) (Fig. 2B) confirmed the shape of the voltammograms according the scheme proposed in Scheme 2. The instability of the radicals has been taken into account: the kinetic constant, k, ($0.1\ s^{-1}$) for the radical-anion A^- is five hundred times greater than that of AH. In the case of the protonation, the kinetic constant k_H (pseudo first order rate $1\ s^{-1}$) for the radical-anion A^- is a thousand times greater than that of A. The radical-anion A^- is nearly a strong base which explains the weak peak current ($Ep \sim 0.4$ V) on the reverse scan. The difference in the acidity properties is in agreement with the potential shift of the redox couples A/A^- and AH^+/AH as in Pourbaix's diagrams.

Previous studies have demonstrated that the antiplasmodial property of the INODs was controlled by a bioreductive transformation in RBCs [6], with the compounds being immediately reduced when entering the RBC by a pathway that is thiol- and enzyme-dependent. Some thiol reagents, like mercaptoethanol [12], cysteine or *N*-acetylcysteine mimic the reactivity of thiol-containing enzymes, such as topoisomerase [12,13]. To study the interaction of the compound with such thiol-containing enzymes, the electrochemical behavior of compound **1** was studied in presence of L-Cys. As shown in Fig. 5A, increasing the concentration of L-Cys resulted in a decrease in the first reduction wave proportional to the concentration added, whereas the oxidation wave remained unchanged. Above 0.75 mM L-Cys, the two reduction waves had almost totally disappeared. The decrease in peak intensity was also accompanied by a peak potential shift to the more positive region. The decline of peak potential and intensity associated to a change of color of the solution indicated that there was a chemical reaction between compound **1** and L-Cys. This result is confirmed by the disappearance of the EPR signal after reduction in presence of L-cysteine (Fig. 3B). The effect of GSH, the most abundant RBC non-protein thiol, is shown in Fig. 5B. In this latter case, there was a greater decrease in the intensity of the reduction waves with a concomitant displacement to low potential.

The same behavior has been described for quinone compounds [13], where 1,2- and 1,4-Michael-type adducts are formed by the addition of the thiol group to the quinone ring. The pseudo-quinone structure of the INOD could explain the similar reactivity towards L-Cys. It was also reported that L-Cys can directly interact with artemisinin (without iron mediation) to form a binary adduct, enhancing artemisinin stability with subsequent negative shift of the reduction potential from -0.64 V to -1.03 V [14]. The decrease in the peak intensity recorded in our case, with the subsequent potential shift, may be due to a reaction of INOD with thiols.

3.2. Chemical analysis of the interaction between compound **1** and L-Cys

Chromatographic analysis of the products obtained from the chemical interaction between compound **1** and L-Cys in solution is shown in Fig. 6. The reaction between compound **1** and L-Cys leads to the reduction of the nitrone function moiety (C═NO) and the formation of three major products (P1, P2, and P3) as shown in Fig. 6. As the parent compound **1** ($t_r = 18.7$ min) is chlorinated, therefore the follow-up of its

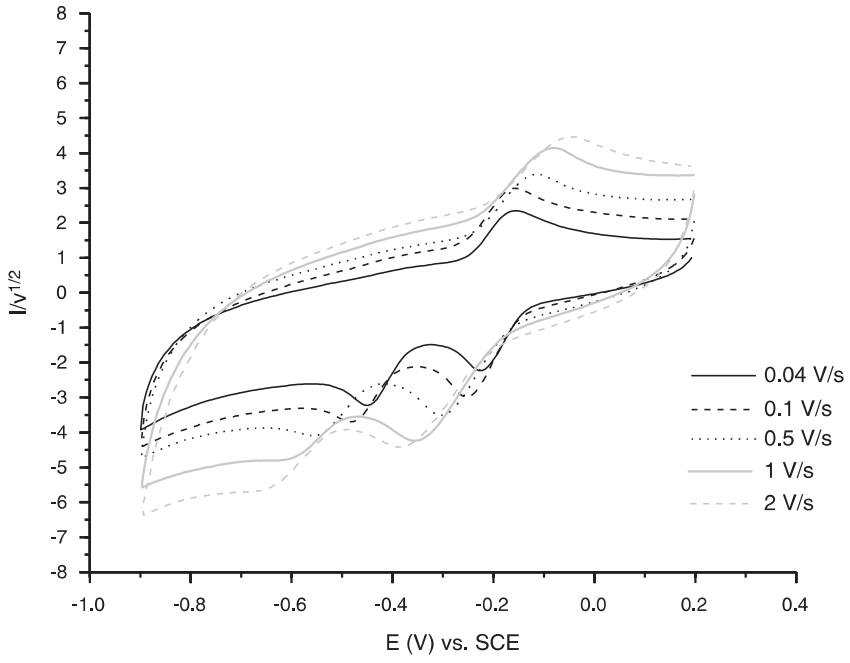

Fig. 4. Normalized cyclic voltammograms at a glassy carbon electrode (1 mm diameter) in DMSO/water (80/20, v/v) of compound **1** at different potential scan rates v; the current is normalized by $I/v^{1/2}$.

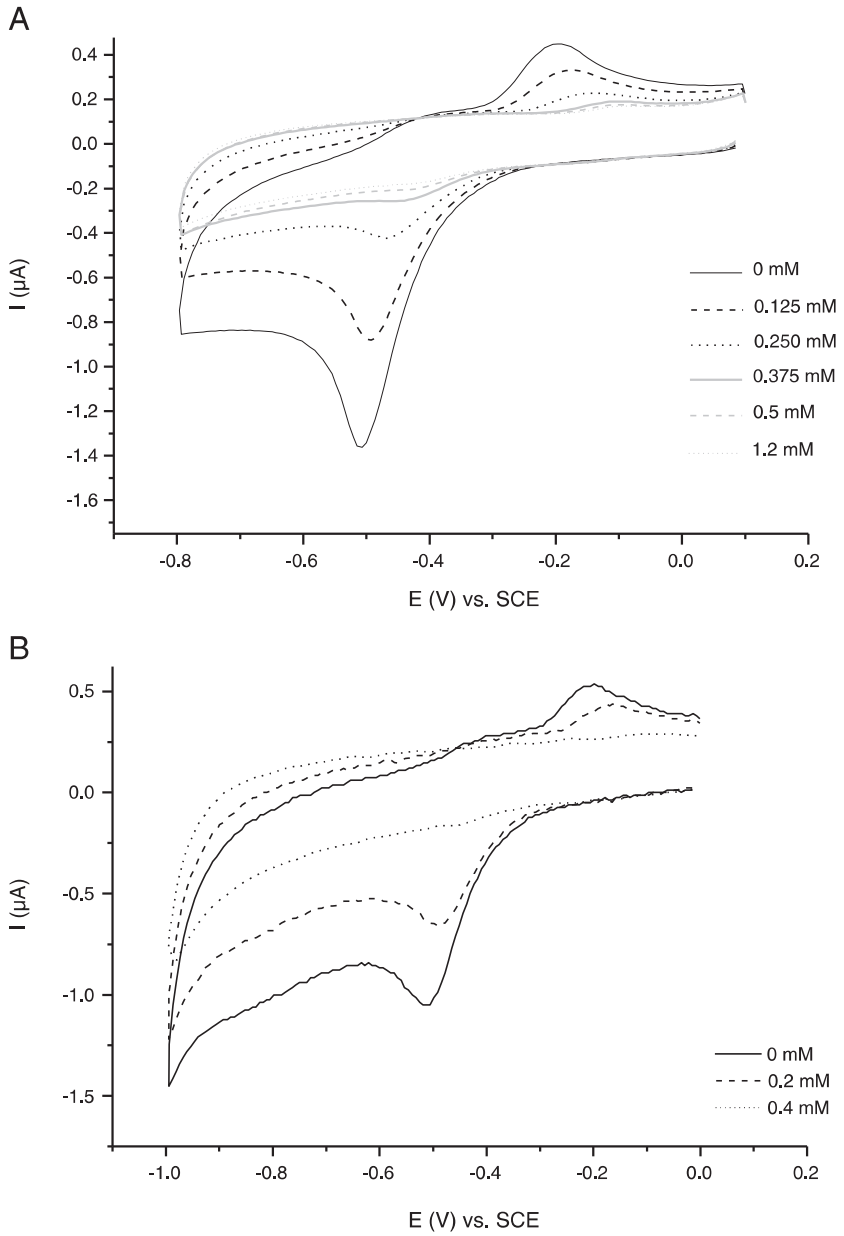

Fig. 5. Cyclic voltammograms of compound **1** (0.25 mM) at a glassy carbon electrode in presence of various concentration of (A) L-cysteine and (B) GSH recorded in DMSO/phosphate buffer (80/20, v/v), pH = 7.

products (P1, P2, and P3) is favored by mass detection. These three major products had different UV–Vis spectra with masses of 303, 303, and 319 amu for P1, P2, and P3, respectively. This suggests that two reduced (dihydrogenated) isomers (303 amu) and a hydrated form (319 amu) are produced. Of particular interest is the product P1, eluted at t_r = 9.7 min, with the reduced nitrone moiety (C(OH) – NH). It corresponds to the same compound isolated from human erythrocytes when compound **1** was incubated inside these cells [6]. The second product, P2, (t_r = 11.0 min) may correspond to another reduced form (C(H) – NOH) whereas the third product, P3, (t_r = 17.5 min) may correspond to (C(OH) – NOH). These three forms are in agreement with the reduction and hydration reactions known for the nitrone moiety [15].

3.3. Reactivity of compound 1 towards Fe(II)-heme and Fe(III)-hemin

In infected RBC, the parasite responsible for malaria digests the hemoglobin to use the amino acids to its advantage. In the course of this hemoglobin digestion, four equivalents of [Fe(II)-heme] are released and oxidized into hematin which is detoxified by the parasite into the malaria pigment or hemozoin, a highly insoluble microcrystalline form of [Fe(III)(protoporphyrin-IX)]. One mechanism proposed for the quinoline-type antimalarial drugs, such as CQ, quinacrine, quinine, and mefloquine is that they exert their action by disrupting the formation of the hemozoin pigment, thus eliciting toxicity to the parasite from the build-up of free heme [15,16]. Studies suggested that the interaction of these drugs with ferriprotoporphyrin-IX occurred through coordination of the amino-quinoline group of the drug to the iron center [17,18]. Therefore it appeared interesting to study the interaction of compound **1** with iron heme model complexes in solution using EPR spectroscopy, to compare with artemisinin and chloroquine. The paramagnetic monomeric hemin complex, [Fe(III)-hemin] presents, at 107 K (liquid nitrogen flow), a single EPR asymmetrical broad line at g = 5.656 characteristic of a ferric high-spin complex (S = 5/2) [19,20] (Fig. 7a). Adding compound **1**, ART, CQ or quinine (Q) to the medium containing the hemin complex, did not change the EPR spectra (Fig. 7b, c, d and e).

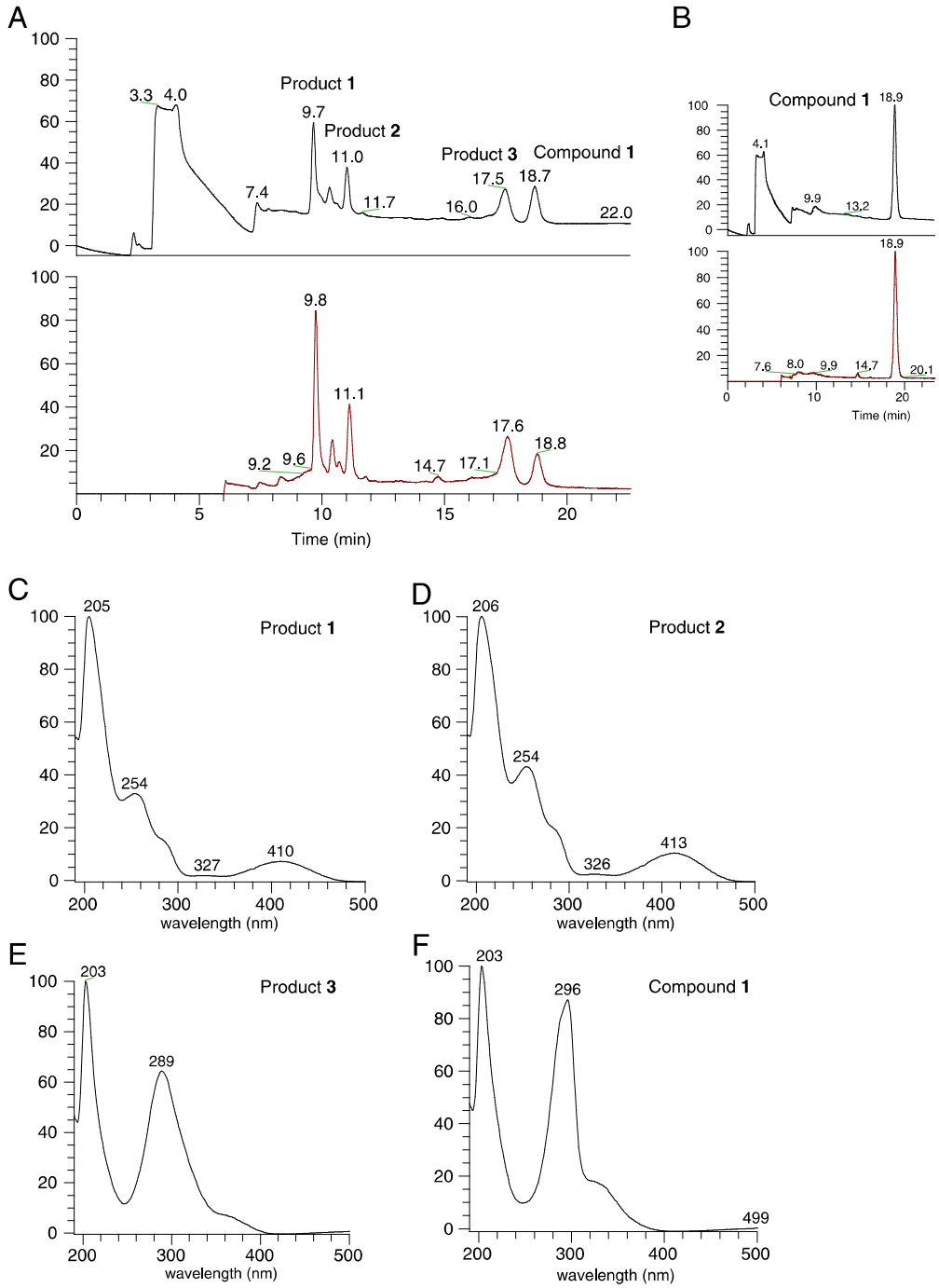

Fig. 6. LC-(-)APCI–MS analysis of A) the interaction between compound **1** (0.25 mM) and L-Cys (2.5 mM), the top chromatogram was obtained from a photodiode array detector (total scan) and the bottom chromatogram obtained from (-)APCI-MS (total ion current); B) the same as (A) but without L-Cys; C), D), E), and F) represent the corresponding UV–Vis spectra of each compound.

In a second step, hydroxylamine ($NH_2OH.HCl$) was added to the hemin complex solution (Fig. 7f). A large decrease of the EPR signal intensity was observed under these conditions indicating a loss of the paramagnetic properties of the sample. The lack of any new EPR lines on the spectra and this strong decrease in intensity are in favor of the formation of the hematin μ-oxo-dimer (μ[Fe(III)PPIX]$_2$O) from hemin [21,22]. This dimer does not yield an EPR signal due to an antiferromagnetic coupling between the two S = 5/2 ferric ions. This spin state has been proposed from susceptibility measurements and Mössbauer studies [21,22]. When compound **1** or ART is added to the mixture under these conditions, the same weak intensity line is observed (Fig. 7g and h, respectively) showing that the EPR silent species (μ-oxo dimer proposed) is not modified in its ligand coordination and spin state. It is completely different when CQ is added to the mixture since there are no traces of high spin iron(III) at g = 5.656 but a strong and unique signal appears at g = 2.026 (Fig. 7i). The same result was obtained with quinine (Fig. 7j). Antimalarial drugs such as chloroquine and quinine are known to exert their antimalarial activity by binding to hematin in its μ-oxo-dimer form, avoiding the formation of hemozoin [23]. Interaction of the hematin μ-oxo dimer with CQ and Q could modify the redox and spin state of the metal ion. The line observed at g = 2.026 could then correspond, as described in

literature [24,25], to an oxidized form of the μ-oxo form dimer (μ-[PPIXFe(III)-O-Fe(IV)PPIX(L)$_x$]) (L = CQ or Q) which is paramagnetic. Whatever the EPR silent species formed by adding hydroxylamine (μ-oxo dimer hypothesized), only chloroquine and quinine are able to change the iron coordination and spin state of this species showing that they enter the coordination sphere of the metal while compound **1** and artemisinin cannot. These results show that the mechanism of action of these indolone-*N*-oxides does not lie in their ability to interact with an iron center to prevent the biocrystallization of hemozoin.

3.4. Interaction of INOD with radicals derived from artemisinin and iron

Our results on fresh clinical isolates showed a slight synergistic action between artemisinin and INODs [2]. The key pharmacophore of INODs is the indolone-*N*-oxide core (conjugated nitrone function) which may trap radicals [26] and the key pharmacophore of artemisinin is the endoperoxide bridge [27] which may produce radical species with iron(II) [16,18]. Iron(II) salts reductively activate the peroxide bond of artemisinin leading to the formation of a pair of oxyl radical intermediates that rapidly rearrange via either a 1,5 H-shift or β-scission to produce the more stable carbon-centered radicals [28]. These alkyl radicals can be readily formed in vivo by the reaction of artemisinin with iron(II)-heme [16,29,30], the most abundant source of iron in Plasmodial-infected erythrocytes. It is proposed that these reactive C-radicals interact with cellular components such as heme and parasite proteins resulting in the death of the parasite. Because of these opposite properties between INOD and artemisinin, the possibility that compound **1** or its reduced form, may or may not trap the radicals generated by artemisinin in the presence of iron(II), has been studied using EPR to understand the synergistic effect recorded in our case. The EPR spectrum obtained from the mixture compound **1**/artemisinin/iron(II) is

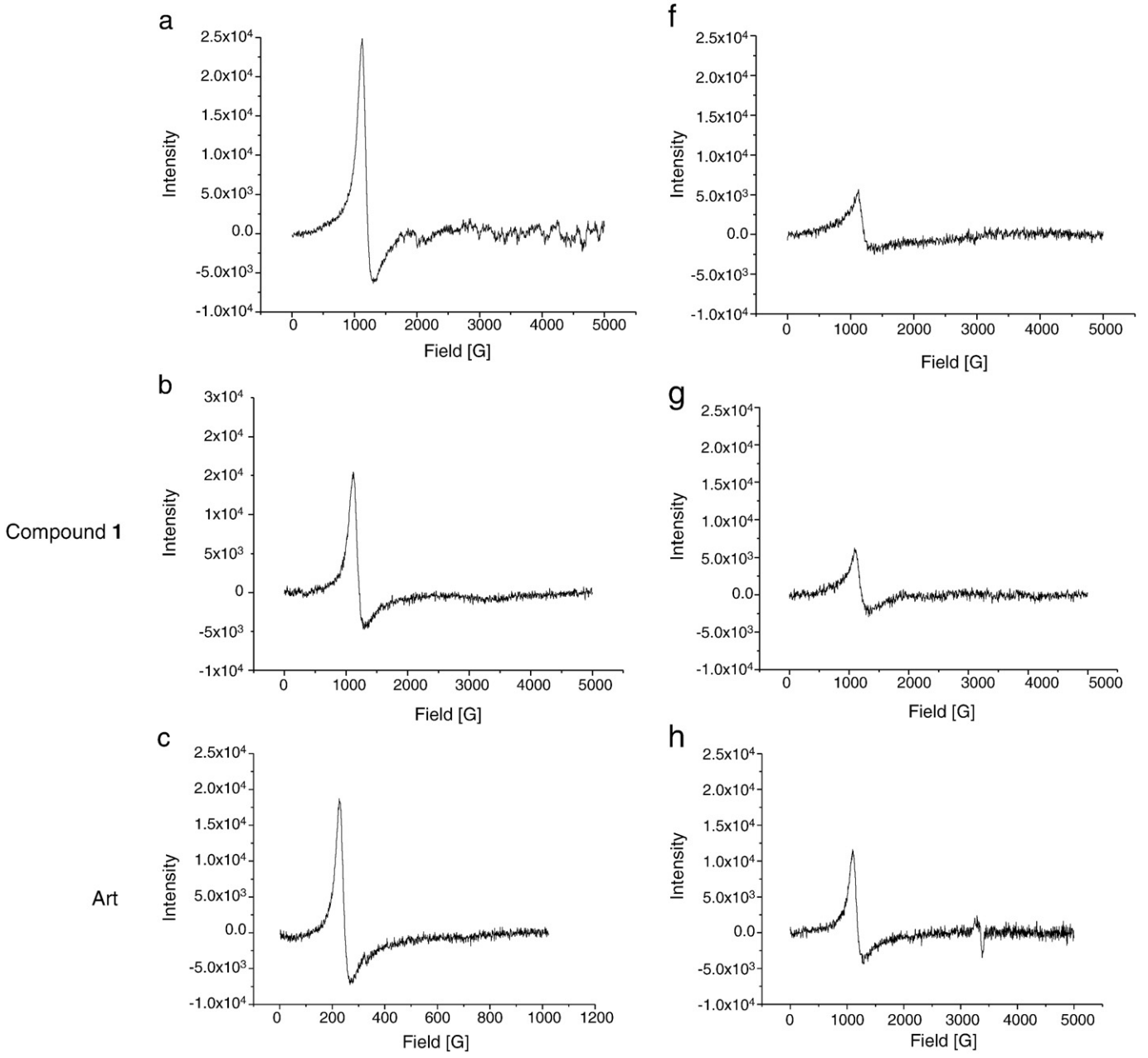

Fig. 7. EPR spectra recorded in frozen DMSO at 107 K with a) hemin (0.75 mM), b) hemin/compound 1 (0.75/3 mM), c) hemin/artemisinin (0.75/3 mM), d) hemin/chloroquine (0.75/3 mM), e) hemin/quinine (0.75/3 mM), f) hemin/hydroxylamine (0.75/7.5 mM), g) hemin/hydroxylamine/compound **1** (0.75/7.5/3 mM), h) hemin/hydroxylamine/artemisinin (0.75/7.5/3 mM), and i) hemin/hydroxylamine/chloroquine (0.75/7.5/3 mM), j) hemin/hydroxylamine/quinine (0.75/7.5/3 mM).

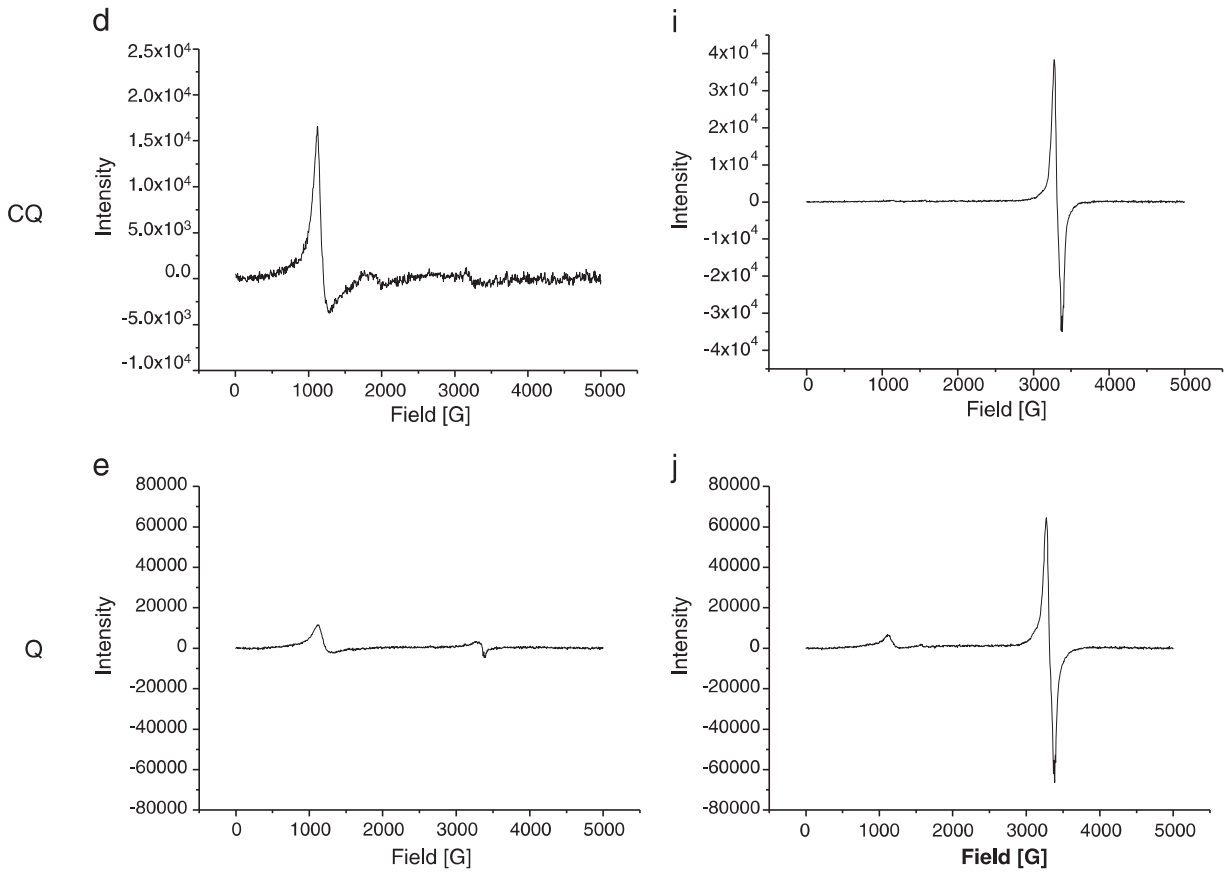

Fig. 7 (*continued*).

presented in Fig. 8A. The EPR spectrum consists of a six-lined spectrum characterized by the hyperfine splitting constants: a_N = 9.57 G; a_H = 2.50 G. In the absence of iron(II) and/or artemisinin, no EPR spectrum was recorded. The results confirm that the INOD compound can efficiently trap the "iron-mediated" artemisinin radicals, whereas INOD did not generate any radicals in the presence of Fe(II), under our experimental conditions (Fig. 8B). On the contrary, after reduction of compound **1**, no trapped radicals were observed on the EPR spectrum (Fig. 8C). This result is in contradiction with the synergic effect recorded for the two drugs and demonstrates that the mechanism of action of compound **1** do not lie on its radical trapping properties.

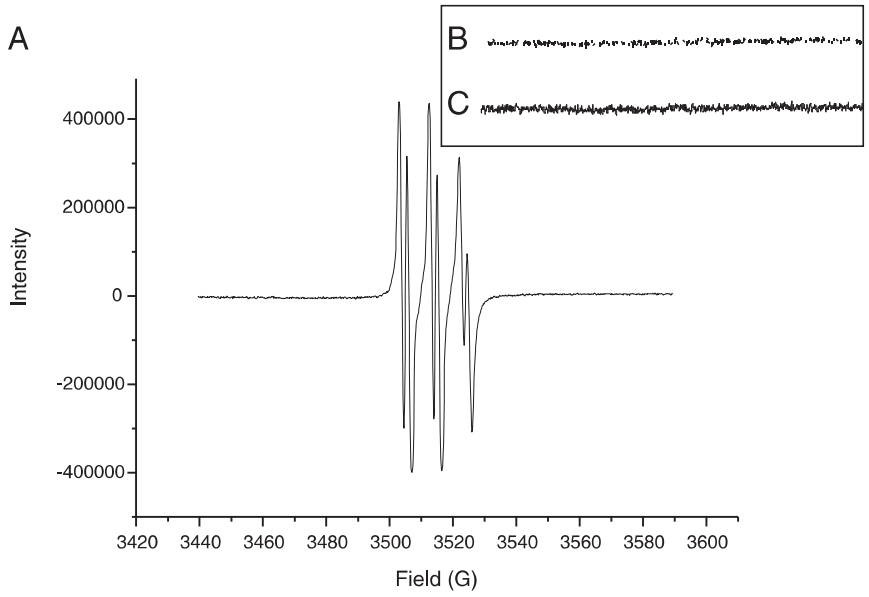

Fig. 8. EPR spectra recorded after 10 min incubation in DMSO/water (90/10, v/v) of a mixture containing A) artemisinin 2.5 mM, Fe^{2+} ($(NH_4)_2Fe(SO_4)_2.6H_2O$) 0.25 mM and compound **1** (0.25 mM); (inset, B) Compound **1** and Fe^{2+}; (inset, **C**) compound **1**/Fe^{2+}/ART/L-Cys.

4. Conclusion

These results show that compound **1** i) does not enter the coordination sphere of the metal in the iron complex as does chloroquine; ii) cannot trap free radicals after reduction; iii) generates stable free radical adducts after reduction at one electron. These results are in good agreement with the fact that no correlation was observed between INODs and chloroquine responses on fresh clinical isolates of *P. falciparum* [2] while in vitro the responses of compound **1** and artemisinin were significantly and positively correlated. The results suggest different mechanisms of action or different molecular targets for these three antimalarial drug classes. These hypotheses are reinforced by the fact that INODs are equipotent against both types of chloroquine resistant and sensitive strains of *P. falciparum* [1,2] INODs lose radical trapping properties after reduction which happens via a rapid intracellular erythrocytic thiol-dependent reduction as reported previously [6]. These results confirm that the bioactivity of INODS compounds does not lie in their spin-trapping properties but rather in their pro-oxidant character. This property may initiate the redox signal that activates SYK kinases and induces a hyperphosphorylation of AE1 (band 3) and could be connected to the pro-oxidant effects of both derivatives but with different targets [5].

Abbreviations

INODs	indolone-*N*-oxide derivatives
P. f.	*Plasmodium falciparum*
DMF	dimethyl formamide
CQ	chloroquine
ART	artemisinin
SCE	saturated calomel electrode
LC-MS	Liquid chromatography–mass spectrometry
RBC	red blood cell

Acknowledgment

This work was supported by the European Commission (FP6-LSH-20044-2.3.0-7, STREP no. 018602, Redox antimalarial Drug Discovery, READ-UP), IDEALP'Pharma and the French Research National Agency (ANR-10-BLAN-0726, Mechanisms of action and Targets of new antimalarial Redox molecules, MATURE). We thank J.-P. Nallet for scientific contribution.

References

[1] F. Nepveu, S. Kim, J. Boyer, O. Chatriant, H. Ibrahim, K. Reybier, M.-C. Monje, S. Chevalley, P. Perio, B.H. Lajoie, J. Bouajila, E. Deharo, M. Sauvain, R. Tahar, L. Basco, A. Pantaleo, F. Turini, P. Arese, A. Valentin, E. Thompson, L. Vivas, S. Petit, J.-P. Nallet, J. Med. Chem. 53 (2010) 699–714.
[2] R. Tahar, L. Vivas, L. Basco, E. Thompson, H. Ibrahim, J. Boyer, F. Nepveu, J. Antimicrob. Chemother. 66 (2011) 2566–2572.
[3] J.E. Bunney, M. Hooper, J. Chem. Soc. B 7 (1970) 1239–1241.
[4] D.N. Polovyanenko, V.F. Plyusnin, V.A. Reznikov, V.V. Khramtsov, E.G. Bagryanskaya, J. Phys. Chem. B 112 (2008) 4841–4847.
[5] A. Pantaleo, E. Ferru, R. Vono, G. Girbaldi, O. Lobina, F. Nepveu, H. Ibrahim, J.-P. Nallet, F. Carta, F. Mannu, P. Pippia, E. Campanella, P.S. Low, F. Turrini, Free Radic. Biol. Med. 52 (2012) 527–536.
[6] H. Ibrahim, A. Pantaleo, F. Turrini, P. Arese, J.-P. Nallet, F. Nepveu, Med. Chem. Commun. 2 (2011) 860–869.
[7] H. Cerecetto, M. González, Mini-Rev. Med. Chem. 1 (2001) 219–231.
[8] K. Reybier, T.H.Y. Nguyen, H. Ibrahim, P. Perio, A. Montrose, P.-L. Fabre, F. Nepveu, Bioelectrochemistry 88 (2012) 57–64.
[9] T.J. Egan, D.C. Ross, P.A. Adams, FEBS Lett. 352 (1994) 54–57.
[10] S.R. Meshinik, T.E. Taylor, S. Kamchonwongpaisan, Microbiol. Rev. 60 (1996) 301–315.
[11] G.L. McIntire, H.N. Blount, H.J. Stronks, R.V. Shetty, E.G. Janzen, J. Phys. Chem. 84 (1980) 916–921.
[12] K. Neder, L.J. Marton, L.F. Liu, B. Frydman, Cell. Mol. Biol. 44 (1998) 465–474.
[13] A.M. Oliveira-Brett, M.O.F. Goulart, F.C. Abreu, Bioelectrochemistry 56 (2002) 53–55.
[14] Y. Pei-hui, S. Zhang-yi, Z. Zhi-jun, C. Ji-ye, H. Qing-yu, J. Chin. Clin. Med. 1 (2006) 21–26.
[15] J. Hamer, A. Macaluso, Chem. Rev. 64 (1964) 473–495.
[16] D.S. Bohle, B.J. Conklin, D. Cox, S.K. Madsen, S. Paulson, P.W. Stephens, G.T. Yee, Am. Chem. Soc. Symp. Ser. 572 (1994) 497–515.
[17] In: L. Tilley, P. Loria, M. Foley, P.J. Rosenthal (Eds.), Antimalarial Chemotherapy, Humana Press, Totowa, NJ, 2001, pp. 87–122.
[18] M. Asghari-Khiavi, J. Vongsvivut, I. Perepichka, A. Mechler, B.R. Wood, D. McNaughton, D.S. Bohle, J. Inorg. Biochem. 105 (2011) 1662–1669.
[19] T.J. Egan, R. Hunter, C.H. Kaschula, H.M. Marques, A. Misplon, J. Med. Chem. 43 (2000) 283–291.
[20] D.J.E. Ingram, J.E. Bennett, Discuss. Faraday Soc. 19 (1955) 140–146.
[21] T.H. Moss, R.H. Lifienthal, C. Moleski, G.A. Smyth, M. McDonnel, W.S. Caughey, J. Chem. Soc. Chem. Commun. 5 (1972) 263.
[22] M.A. Torrens, D.K. Straub, L.M. Epstein, J. Am. Chem. Soc. 94 (1972) 4160–4162.
[23] S.R. Vippagunta, A. Dorn, R.G. Ridley, J.L. Vennerstrom, Biochim. Biophys. Acta 1475 (2000) 133–140.
[24] K.M. Kadish, G. Larson, D. Lexa, M. Momenteau, J. Am. Chem. Soc. 97 (1975) 282–288.
[25] R.H. Felton, G.S. Owen, D. Dolphin, A. Forman, D.C. Borg, J. Fajer, Ann. N. Y. Acad. Sci. 206 (1973) 504–515.
[26] J. Boyer, V. Bernardes-Genisson, V. Farines, J.-P. Souchard, F. Nepveu, Free Radic. Res. 38 (2004) 459–471.
[27] D.L. Klayman, Science 228 (1985) 1049–1055.
[28] G.H. Posner, C.H. Oh, J. Am. Chem. Soc. 114 (1992) 8328–8329.
[29] Y.L. Hong, Y.Z. Yang, S.R. Meshnick, Mol. Biochem. Parasitol. 63 (1994) 121–128.
[30] A. Robert, J. Cazelles, B. Meunier, Angew. Chem. Int. Ed. 40 (2001) 1954–1957.